Article

Peculiarities of Dynamics of Hypergenic Mineral Transformation of Nickel Weathering Crusts of Ultramafic Rocks of the Kempirsay Group of Deposits in Western Kazakhstan

Valeriy Korobkin [1,*], Iskander Samatov [1,2], Akhan Chaklikov [1] and Zhamal Tulemissova [1]

[1] Faculty of Geology and Geological Exploration, Kazakh-British Technical University, Almaty 050000, Kazakhstan; samatov.40@mail.ru (I.S.); a96chaklikov@gmail.com (A.C.); ztulemissova@gmail.com (Z.T.)

[2] Institute of Geological Sciences Named Satpayev K.I., Almaty 050010, Kazakhstan

* Correspondence: korobkin_vv@mail.ru; Tel.: +7-(727)-399-9292

Abstract: Nickel weathering ores are used to produce metallic nickel, stainless steels, and nickel sulfate, the main component of batteries. The global production of nickel from weathering ores is increasing and has surpassed production from sulfide magmatic deposits. The efficiency of the mining and processing of nickel ores from weathering rocks is determined by their mineralogical composition. The weathering crust profile of the Kempirsay ultramafite massif is divided into three zones—leached (kerolitized) serpentinites, nontronites, and final hydrolysis minerals (later referred to as "ochers"). The kerolitized zone consists of a mixture of Ni-bearing talc and saponites (later referred to as "kerolite"). During the geological mapping of the Donskoye, Buranovskoye, and Shelektinskoye deposits, the products of ultramafite hypergenic transformation into disintegrated and leached serpentinites, kerolites, nontronites, and ochers were selected and studied. For this purpose, 44 rock samples were studied via X-ray diffractometric and thermal analyses, supplemented with data from chemical, microscopic, and granulometric determinations. Based on the obtained numerical parameters of the crystalline structure of the weathering products, the thermochemical values were obtained. The hypergenic transformation of the initial minerals and their subsequent transformation were traced. The trace element distribution along the profile of the serpentinite weathering ores is related to the initial material composition of the ultramafites. The accumulation of nickel in industrial concentrations is associated with the nontronite–kerolite zone. X-ray diffractometric analysis can be used as a fast and reliable method for controlling the nickel content of ores and monitoring their mineralogical composition.

Keywords: Kempirsay ultramafite massif; nickel weathering crusts; serpentinite; nontronite; kerolite; nickel ores; thermal analysis; X-ray diffraction analysis

1. Introduction

The systematic study of nickel-bearing weathering crusts in Kazakhstan has been actively carried out since the 1930s. More than 40 industrial deposits and about 30 occurrences of silicate nickel ores have been discovered and explored since then [1–5].

The Mugodzhar ore district covers the western slope of the mountains of the same name and extends to the north, according to the main geological structures, for hundreds of kilometers. The area contains numerous massifs of ultramafic rocks. Within this territory exists the largest massifs of ultramafic rocks in Kazakhstan, which contain ore-bearing weathering crust—Kempirsay and Daul-Kokpekty. Most of the developed deposits of silicate nickel ores from the weathering crusts are located within the Kempirsay massif. In its peripheral parts, near the point of contact with host rocks, the weathering crust remnants

of the main area type have been preserved from denudation. This is where the industrial concentrations of nickel are confined [1–3].

The ore-bearing substrate for hypergenic nickel deposits is serpentinized ultramafites, as well as the serpentinites and metasomatites that develop over them. The hypergene minerals formed in the weathering crust are represented by iron oxide (goethite) and nontronite–chlorite rocks. In the process of hypergenic change, the chemical compositions of the primary endogenous and hydrothermal–metasomatic rocks of the substrate undergo significant reworking, with the migration of the main components, including Ni, and other chemical elements [4]. Clay minerals are the most common and diverse components of nickel-bearing weathering crust. The genesis of clay minerals in weathering crusts remains a hot topic, despite numerous studies and discussions [1–12]. Highly dispersed layered silicates, which form homogeneous and mixed-layered structures, can record the dynamics of crystallochemical transformations during the interaction of a mineral with a changing environment. They can serve as a universal source of information on the physicochemical conditions of weathering.

X-ray powder diffractometry and thermal analysis play leading roles in determining the crystal structure and chemical composition of highly dispersed clay minerals. These methods can be used to study the multicomponent mineral systems of weathering crusts.

In this context, the typomorphic features of real crystalline structures of clay minerals, general regularities of their formation in nickel weathering crusts, and products of their redeposition are revealed.

2. Geological Structure of the Area

The Kempirsay massif of ultramafic rocks has a narrow, elongated shape in the plains, extending to the south. It is 82 km in length and 31.6 km across (Figure 1). The northern part of the massif narrows to 0.6 km, and the total area is 920 km^2. The shape of the massif is close to lopolite, with a concave wavy surface at the base. It is near the meridional deep fault separating the Uraltau from the Magnitogorsk seam zone.
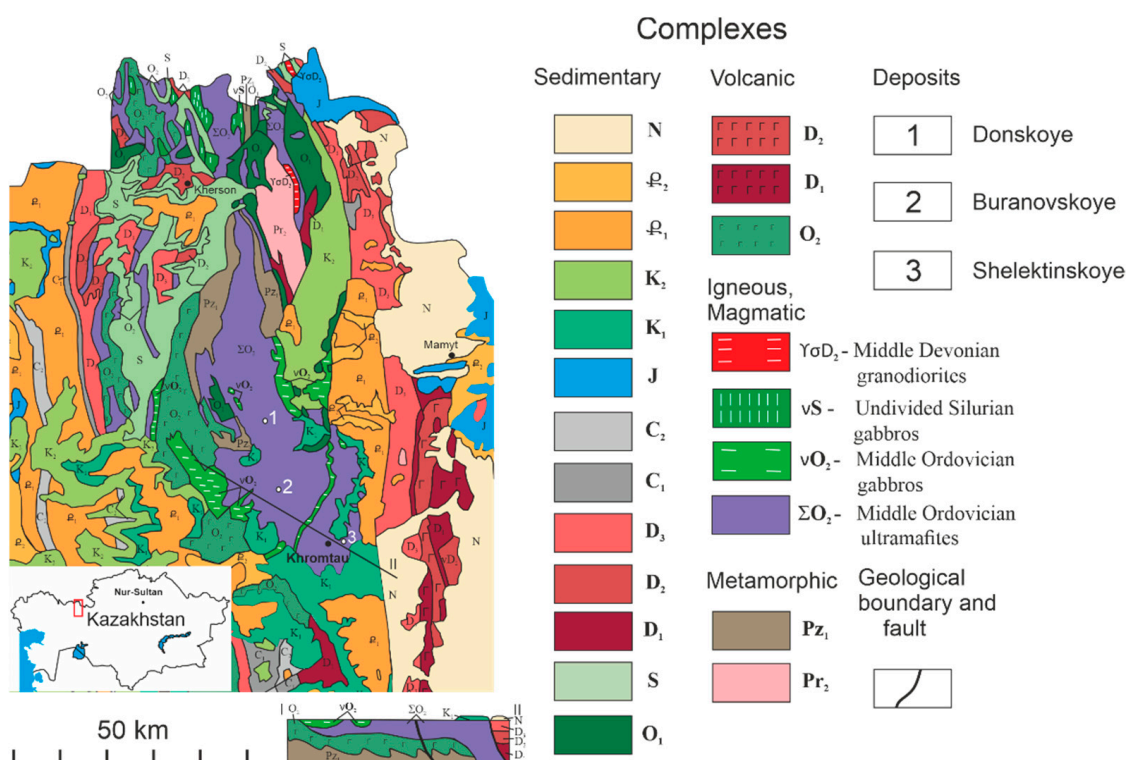

Figure 1. Scheme of the geological structure of the Kempirsay massif of ultramafic rocks [5,6,13].

Ultramafites have tectonic contacts with the Ordovician and Precambrian host rocks. Intervening rocks are composed of sericite–chlorite–quartz, graphitic–siliceous, crystalline Neoproterozoic shales, Ordovician and Silurian effusives, tuffs ranging from basic to acid composition, and Devonian and Devonian–Carboniferous sedimentary rocks (sandstones, siltstones, etc.), as well as sandstones and siliceous shales of the same age (Figure 1). In some places, nickel-bearing weathering crusts of the Kempirsay massif overlap with Lower Cretaceous bauxite-bearing sediments [1–3].

Nickel mineralization is spatially related to the weathering crust developed over serpentinites. The weathering crust remains are zoned and sheltered from the effects of erosion processes on watershed slopes. From the base to the top, the following lithological zones are distinguished: disintegrated and leached nontronitized serpentinites, which are replaced upwards by nontronitic clays, ochers, and ocher–nontronitic formations. According to the results of chemical analysis, all of the lithological varieties of weathering products are industrial ores. Most of the deposits were discovered in the 1930s, during geological mapping, in combination with magnetic and gravity surveying [1–3].

Samples for study and analysis were taken from typical objects of Donskoye, Buranovskoye, and Shelektinskoye deposits (Figures 1–4).
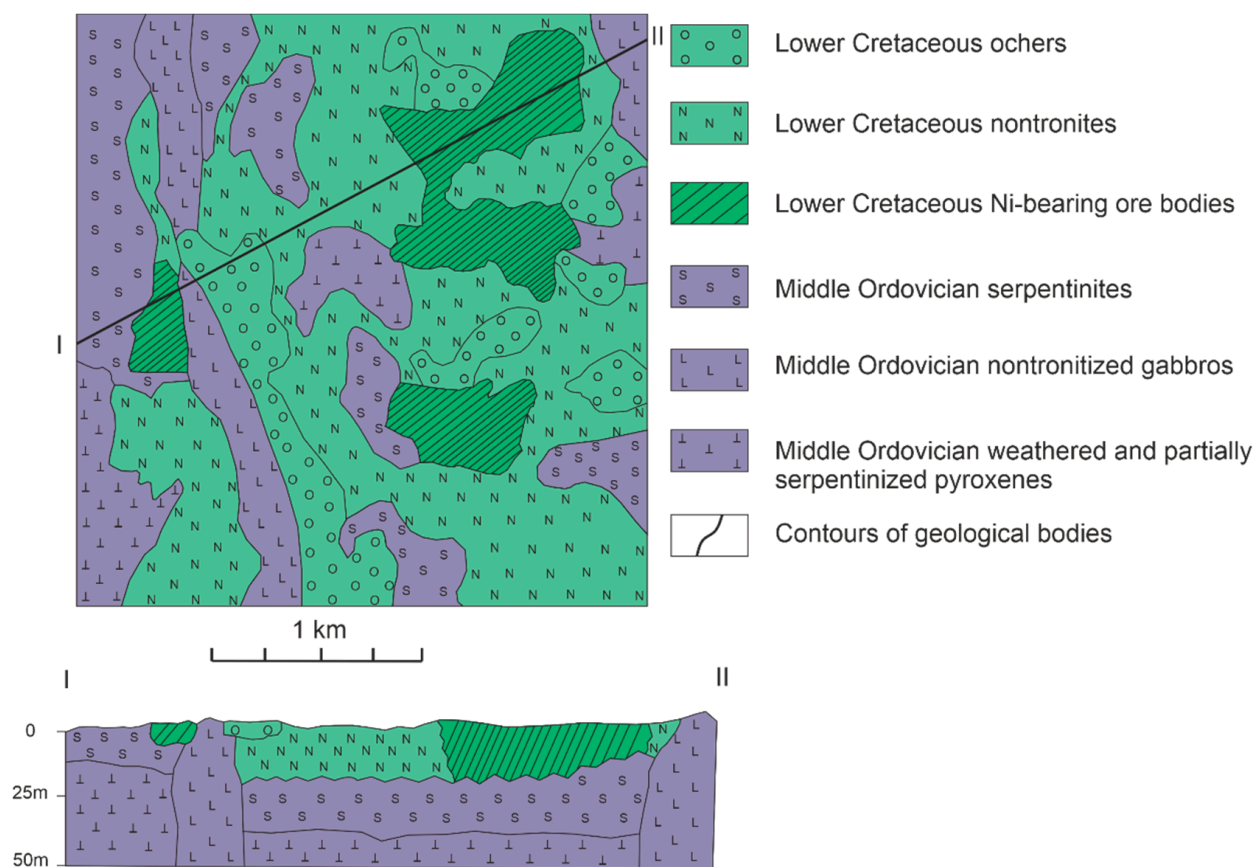

Figure 2. Diagram of the geological structure of the Buranovskoye deposit. Upper (hypergenic) stage—weathering crust. Lower stage—altered ultramafic rocks.
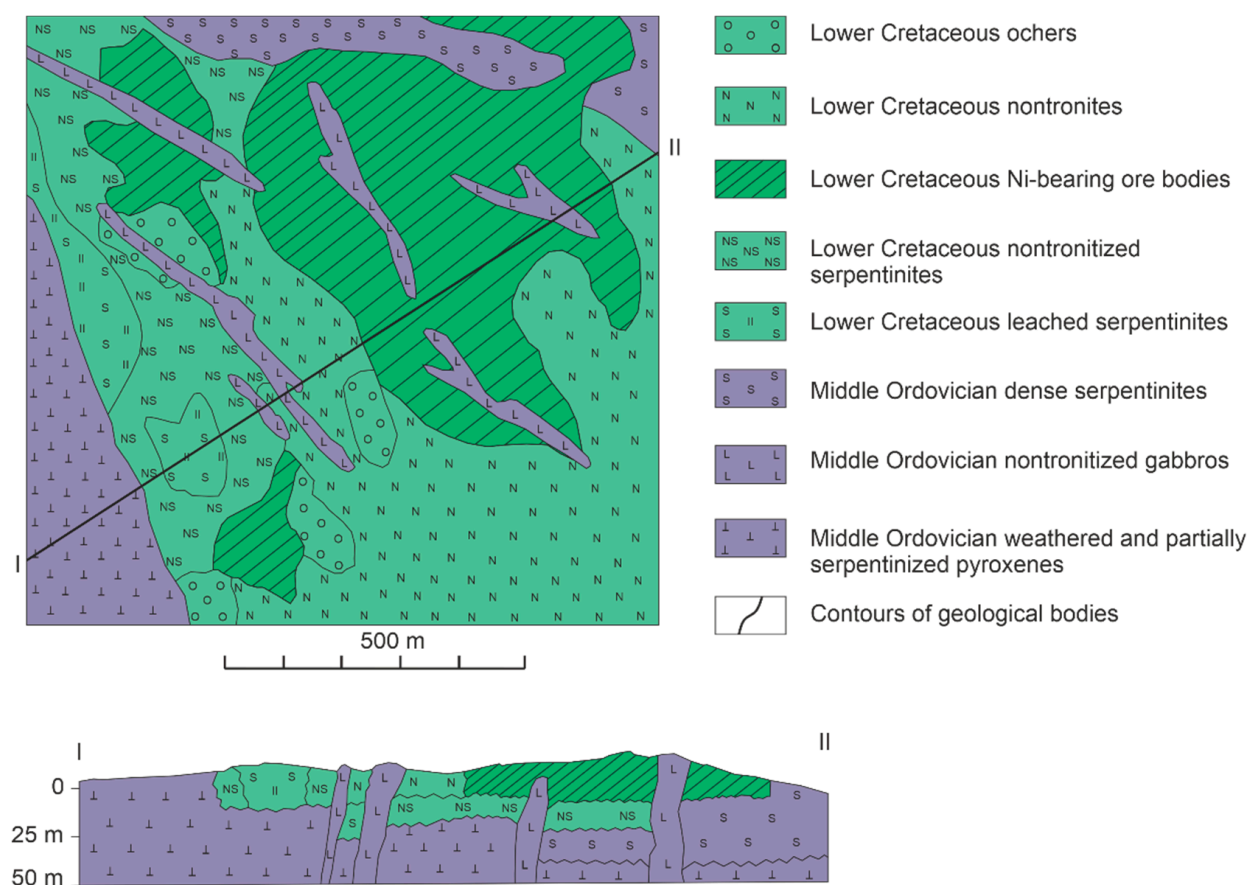
Figure 3. Scheme of the geological structure of the Shelektinskoye deposit. Upper hypergene layer—weathering crust. Lower tier—altered ultramafic rocks.
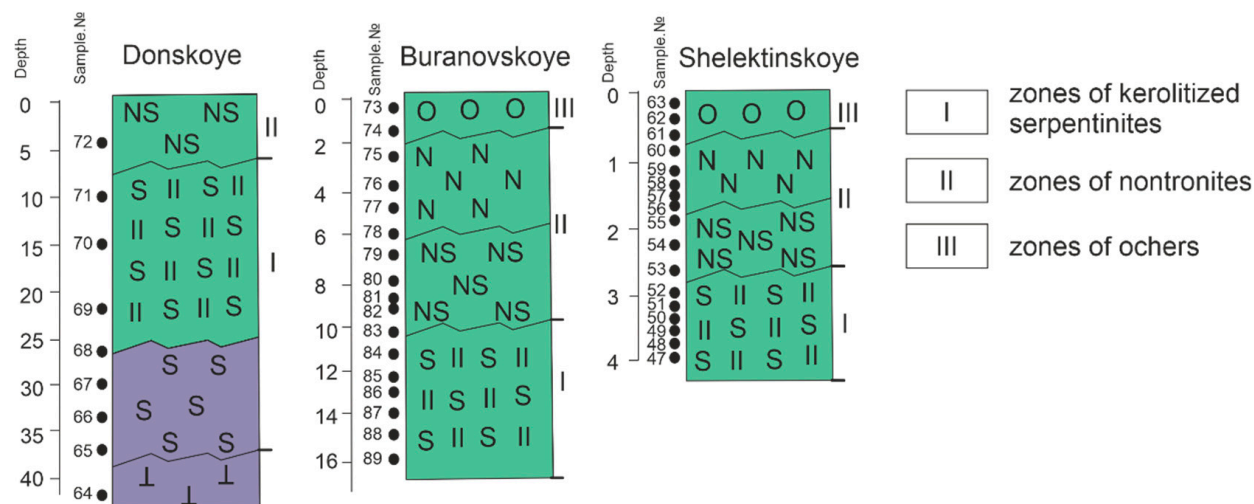
Figure 4. Zones of hypergenic transformation of the weathering rocks of ultramafic rocks Donskoye, Buranovskoye, and Shelektinskoye deposits. Note—symbols in Figure 3.

The Donskoye deposit is composed of altered serpentinites containing chromite mineralization (Figure 1). The ore bodies form a band that is 6 km long and 0.3 km wide. The main ore minerals, magnesiochromite and Cr-bearing hercynite (later referred to as "chrompicotite"), are crystalline in shape and up to 5 mm in size. Total ore reserves of the entire group of deposits weigh 200 thousand tons, with an average chromium oxide content of 47.4% [3].

The Buranovskoye deposit is located in the eastern contact zone of the ultramafic Kempirsay massif (Figure 1). The weathering crust of this deposit has a two-layer structure, in which the hypergene upper layer has a continuation, in the form of the lower hydrothermal layer (Figure 4). The Kempisay massif lies in the overthrust allochthon on the Samara zone of the Mugodzhar. The massif of the ultramafic rocks of the Southern Urals is in Russian territory and occurs in the form of overthrust allochthon [14,15]. All of these ultramafic structural units are under the strong influence of the Main Ural Fault. Taken together, they mark the surface of the detachment and super-regional overthrust cover. The influence of the Main Ural Fault on ultramafic rocks probably affects their hydrothermal alteration [14,15]. Nickel mineralization is located in the weathering crust of gabbro-amphibolites, whose thickness reaches 240 m. The weathering crust is represented by: (1) nontronitized serpentinites and gabbro-amphibolites; (2) leached, silicified serpentinites; and (3) the ocher zone. The three main deposits of commercial nickel ores are identified at the deposit (Figures 2 and 4). The northeast deposit consists of two ore bodies, with lengths along the strike of 310 and 1180 m, widths of 40 and 700 m, and thicknesses from 1 to 23 m. The depth of the ore bodies varies from 0.5 to 14 m. The western deposit consists of three ore bodies up to 450 m long and 30 to 410 m wide. The depth of these ore bodies varies from 0.5 to 21 m. The eastern accumulation consists of three ore bodies, up to 700 m long and 30 to 300 m wide, with an average thickness of 4.2 m and depths from 0.5 to 23 m. The shape of the ore bodies is stratified, and their underside is undulating. The size of the fluctuations of the relative marks of the bottom of the bodies ranges from 10 to 20 m. The ores have dense and earthy textures. The main ore minerals are represented by nontronite, nickel-bearing chlorite, and asbolane (soft psilomelane); the minor ones are falcondoite, baddeleyite, and psilomelane. About 50–80% of the rock volume is represented by nontronite, which is present in all types of ores as continuous clusters. Chlorite occurs as flake aggregates that fill the cracks in the host rocks. Asbolane forms advection crusts and earthy formation, which is often found as dendrites. The average nickel content is 1.11%. The content of the accompanying harmful impurities are copper (0.047%) and chromium oxide (5.35%) [1–3].

The Shelektinskoye deposit is located in the southern part of the Kempirsay massif (Figure 1) and has a two-layer structure. The hypergenic upper tier has a continuation, in the form of the lower hydrothermal tier (Figures 3 and 4). The weathering crust is developed on serpentinites and represented by a reduced profile, which distinguishes a zone of modified nontronitized serpentinites, as well as a zone of ocher. Within the deposit, eight deposits of conditioned ores, uniting 16 ore bodies with a length of 750 m and average thickness from 3 to 7 m, are identified. The depth the top of the ore bodies reaches 19 m. Horizontally-occurring ore bodies in the deposit have a formation-lens shape; their thickness varies widely. The main ore minerals are nontronite and nickel-bearing chlorite; the secondary minerals are kerolite, falcondoite, and asbolane. Nontronite amounts for 50% of the rock volume and chlorite 10–30%. They occur as clusters of scaly green grains. Asbolane forms thin veins in leached serpentinites and dense crusts in rock voids; its quantity in ore reaches 1% [2,3].

3. Research Methods

To prepare the samples for thermal and radiographic analyses, rocks from weathering cores were subjected to particle size separation. Ten fractions (with particle sizes ranging from <0.001 to >1 mm) were separated using the powder sample precipitation method in distilled water (Figure 5I). Hard rocks (hydrous silicates, carbonates, and oxides of various metals) were distilled, separated, and passed through a magnetic separator, if necessary.
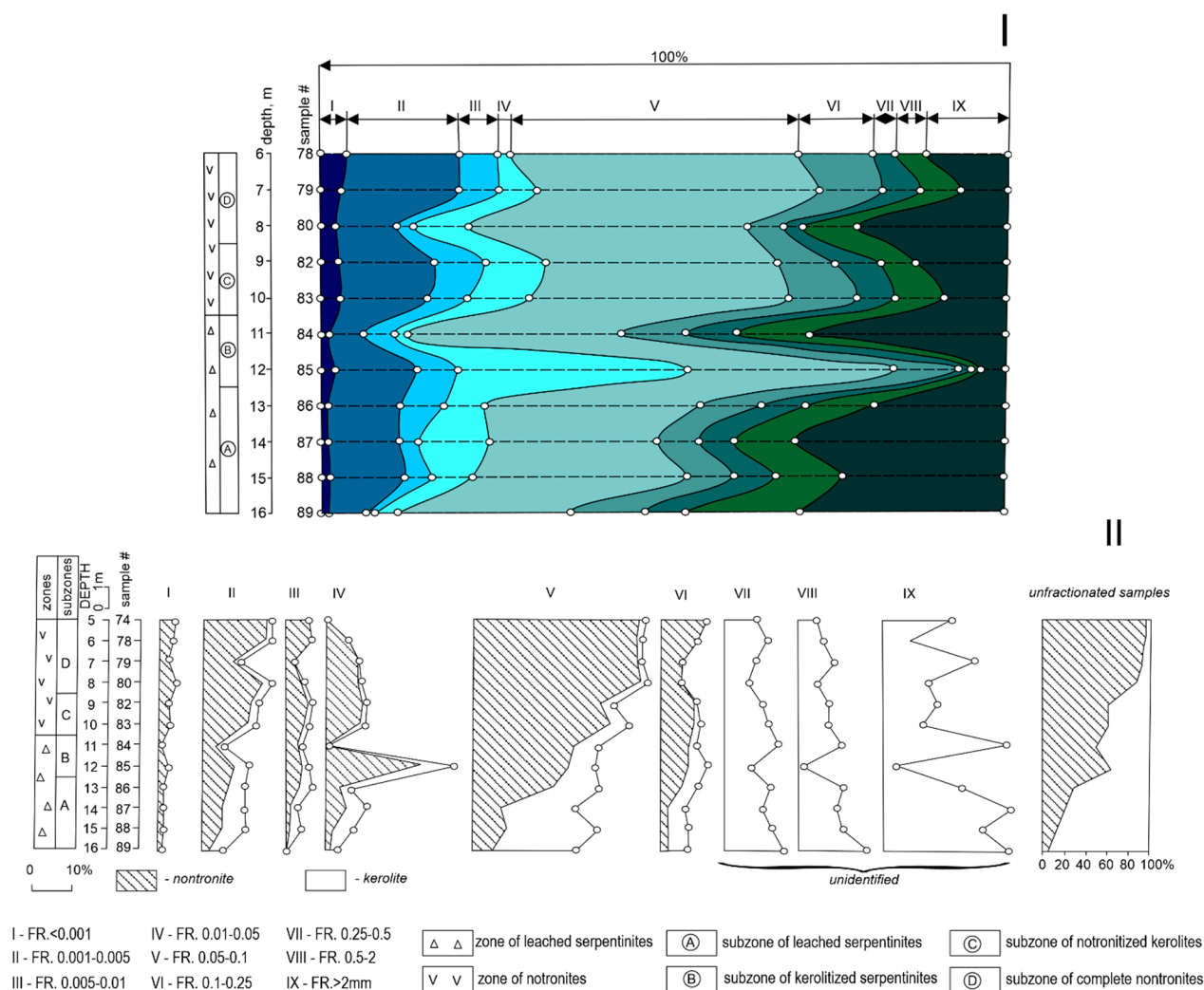
Figure 5. Granulometric spectrum of samples from well 2250 (Buranovskoye deposit, Kempirsay massif, and the lower and middle horizons). (**I**)—variations of the granulometric composition of the products of hypergenesis, depending on the depth of occurrence of rocks. (**II**)—diagrams of the dependence of the distribution of nontronites and kerolites along the weathering profile, regarding the depth of rock sampling and number of fractions.

Core fractionation by particle size was carried out to determine particle sizes that fall within the grain-size spectrum—any mineral into which the studied rocks can be divided. Information about the grain sizes in any fraction of the studied rocks can be used to search the composition of the sample of the assumed mineral, as well as to determine its percentage of content in the rock.

Based on microscopic studies and chemical composition (Figures 4 and 5 and Table 1), all three zones of the nontronite profile of the weathering crust were distinguished. The chemical composition was obtained by complex chemical analysis. The chemical analysis (oxide composition) was selectively controlled on a Superprobe 733 electronic probe micro-analyzer (JEOL, Tokyo, Japan). In the zone of kerolitized (leached) serpentinites, the rocks are dense; they retain the original structure of the parental rocks. Kerolite prevails in the rock mass. Nontronite occurs in the upper part of the zone. Minor amounts of opal, magnesite, calcite, chalcedony, iron, and manganese hydroxides are present here. In the zone of nontronitized serpentinites, nontronite is the main mineral; iron and manganese hydroxides, opal, and chalcedony are present as admixtures. The ocher zone is characterized by the abundance of iron hydroxides, with admixtures of quartz, chalcedony, opal, and nontronite.

Table 1. The chemical composition of the weathering crust of the Kempirsay ultramafite massif [1].

Oxides	1	2	3	4	5	6	7
SiO_2	43.19	41.99	38.37	40.66	39.25	41.13	15.54
TiO_2	0.25	0.30	0.04	0.28	0.31	0.50	0.90
Al_2O_3	3.56	1.62	3.75	3.31	1.89	4.48	5.04
Fe_2O_3	15.98	19.00	32.80	21.33	21.97	21.60	55.20
FeO	0.83	0.42	0.30	0.28	0.33	0.36	0.80
MnO	0.32	0.39	0.70	1.28	0.53	0.70	0.56
MgO	21.25	18.50	5.70	17.20	18.88	5.50	5.75
NiO	0.58	0.87	0.70	0.76	1.16	2.85	0.75
CoO	0.03	0.05	0.05	0.14	0.08	0.09	0.05
P_2O_5	0.04	0.08	0.02	0.05	0.05	0.02	0.18
CO	1.44	0.60	1.40	0.55	0.99	1.14	0.70
H_2O	9.28	13.02	12.93	10.39	10.84	16.81	11.21
Amount	96.75	96.84	96.76	96.23	96.28	96.18	96.68

[1] Note: Buranovskoye deposit (1–3): 1—kerolitized (leached) serpentinites, Zone I (sample 88); 2—leached and kerolitized serpentinites, Zone, Zone I (sample 86) I; 3—leached and kerolitized serpentinites, Zone III (sample 75). The Shelektinskoye deposit (4–7): 4—weakly nontronitized serpentinites, (samples 48–52); 5—intensely nontronitized serpentinites, (samples 51–56), Zone II; 6—nontronites (sample 77), Zone II; 7—ochers (sample 62), Zone III.

Thermal (DTA and TGA) and X-ray phase (XRD) analyses were used as the main methods of the study.

Samples were taken on derivatographs Q-1500D and "C" mark, which allowed us to analyze them in the dynamic heating mode and conditions of quasi-isothermal temperature support in the chamber of the used furnace. At the same time, the following sensitivity levels of the devices were observed: DTA—500 μV/250 mm, DTG—1.0 mV/250 mm, and TG—500 μV/200 mm. Sample weights were 500 mg; the rate of continuous temperature increase was 10 deg/min, and the range of sample calcination was 20–1000 °C. The sensitivity of the analytical scales of the device was 100 mg. Differential thermoanalytical (DTA), differential thermogravimetric (DTG), and thermogravimetric (TG) curves were obtained. The histograms of the curves in each temperature interval reflect the course of thermal degradation of the test sample, accompanied by a change in the enthalpy of the system, as well as a change in the sample mass and its rate of weight loss. On the diffractometer DRON-4, the mineral composition of the samples was revealed, and changes in the perfection of the crystal structure of mineral formations were specified. Using numerical criteria of diffractometry data, changes in the chemical composition (according to the ratio of minerals in the association), as well as the degree of perfection of the crystallographic lattices of minerals, were determined [8–11].

Thermal analysis was carried out on these objects, and DTA, DTG, and TG curves were obtained; their interpretation made it possible to reveal the material composition of rocks and establish the sequence of the formation of secondary minerals in weathering zones.

X-ray measurements were carried out on an automated unit DRON-3 (general purpose X-ray diffractometer), with $Cu_{k\alpha}$-radiation and β-filter. We took diffractograms under the following conditions: U = 35 kV; I = 20 mA; scale: 2000 pulses; time constant 2 s; shooting θ–2θ; and detector 2 deg/min. X-ray phase analysis (XRF) was performed on a semi-quantitative basis on powder sample diffractograms using the equal weight method and artificial mixtures. The quantitative ratios of crystalline phases were determined. The interpretation of the diffractograms was performed using data from the ICDD: powder diffractometric database PDF2 (powder diffraction file) and diffractograms of clean minerals. The possible impurities with ambiguous identification were due to low concentrations and the presence of only 1–2 diffraction reflections, lack of chemical composition data, or poor oxidization. Based on the core material presented by the specified method, the following data were obtained:

1. Interplanar distances and phase composition of samples;
2. Results of semi-quantitative X-ray diffraction analysis;

3. Sample diffractograms.

The above analysis established the mineral composition of the samples and clarified the changes in the perfection of the crystal structure of mineral formations. Using numerical criteria of diffractometry data, the changes in the chemical composition (according to the ratio of minerals in the association) and degree of perfection of the crystal lattice of minerals were determined [8–11].

Thermal analysis in conditions of serpentine heating in temperatures ranging from 20 to 1000 °C yielded thermal curves (Figures 6 and 7), the morphology of which characterizes the degradation dynamics of the tested samples. As seen in the graph (Figure 6), with increasing temperature, the shape of the curves of the heated minerals shows the destruction of the crystal lattice structure. In the temperature ranges of 20–250 °C, 250–440 °C, and 440–800 °C, the rocks studied during dynamic heating displayed endothermic effects, due to the release of adsorbed, interlayer, and crystalline water from the samples, respectively.
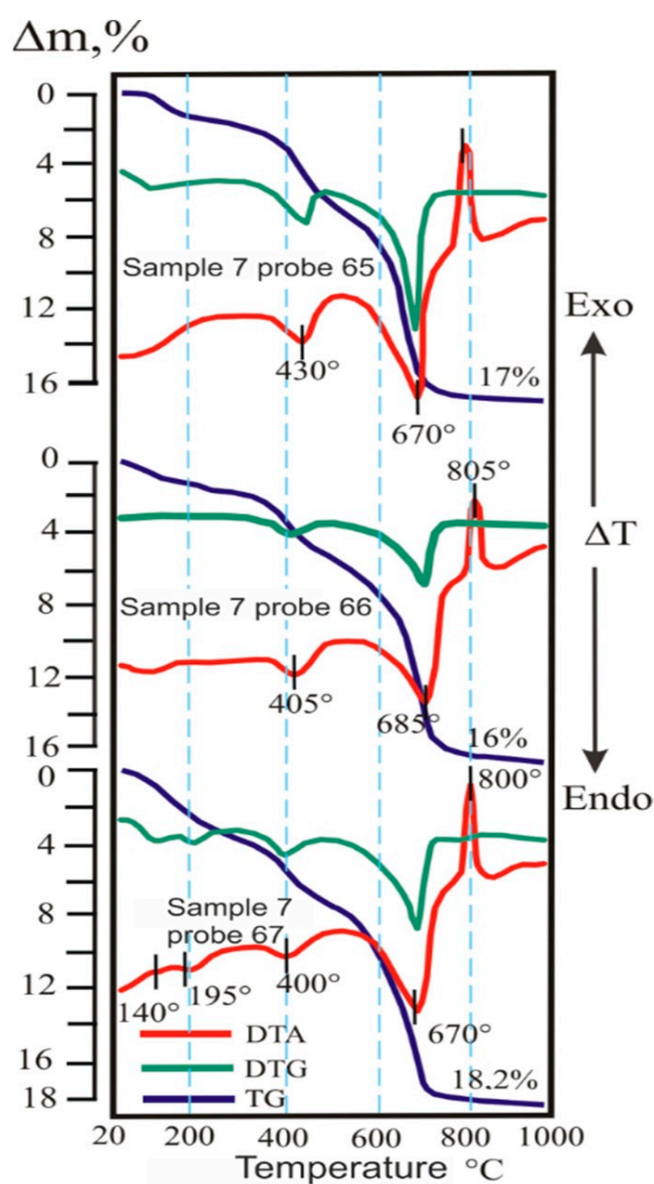

Figure 6. Derivatograms of serpentines of the Donskoye deposit. Exo—exothermic effect, Endo—endothermic effect, ΔT—change in the enthalpy of the system during the thermal transformation of the tested samples.
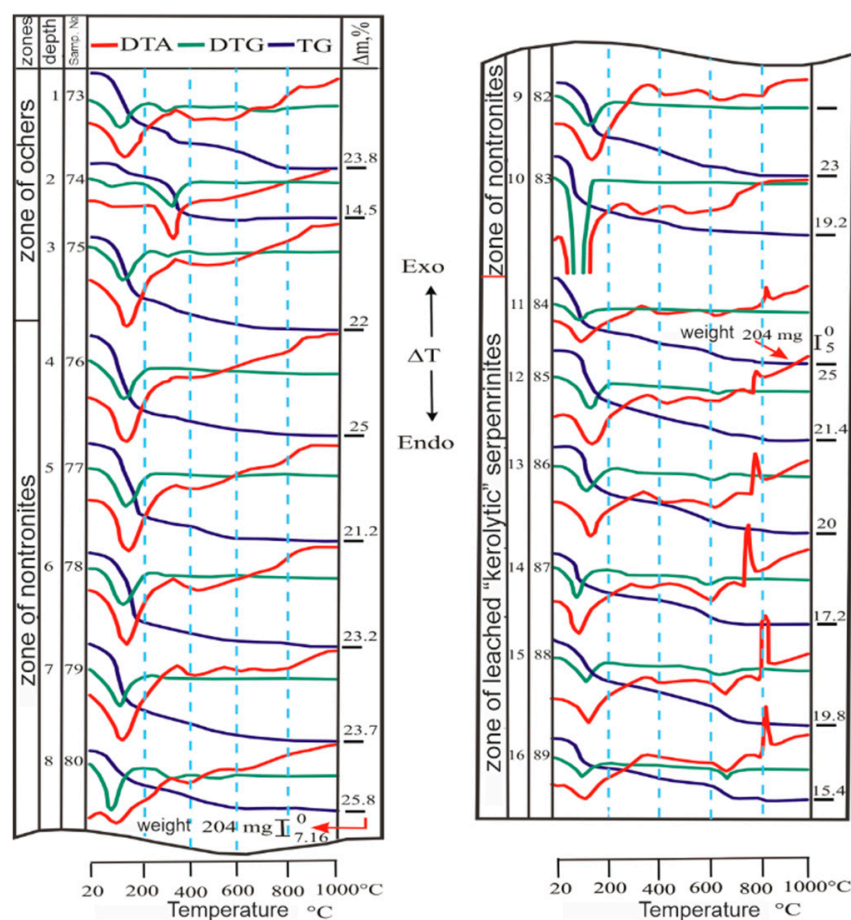
Figure 7. Buranovskoye deposit—serpentine-to-kerolite transformation zone, samples 84–89. Derivatograms of hypergenesis products from weathering crusts of the full profile. DTA—250 µV, DTG—500 µV, TG—100 vu (500 µV), and sample—500 mg. Exo—exothermic effect, Endo—endothermic effect, ΔT—change in the enthalpy of the system during the thermal transformation of the tested samples.

4. The Results Obtained

Using the thermal analysis of the samples from the presented deposits, the thermal curves (DTA, DTG, and TG) were obtained, the morphology of which characterizes the dynamics of the destruction of the host minerals (Figures 6 and 7).

Under the conditions of dynamic heating of serpentinite weathering products, the thermal analysis reveals the material composition of rocks and establishes the boundaries of mineral zones along with the weathering profiles.

The derivatograms of serpentines, which formed the weathering crust of the Donskoye deposit, are shown on the graph (Figure 7). The figure shows that the shape of the thermal curves changes strongly with increasing calcination temperature. This change in the trajectory of the curves in a changing temperature field is caused by serpentine degradation.

Within the temperatures of 20–250 °C, 250–440 °C, and 440–800 °C, sample 65 (during dehydration) first loses 12% (H_2O) of its weight; then, in order of sequence, it reduces its weight (in the form of OH loss) by another 20 and 68%. Samples 66 (11.3, 20, and 68.7%) and 67 (20, 22, and 58%) were dehydrated in the same sequence.

The main mass of hydroxyl water from the serpentine crystal lattice is removed within ~500–780 °C and accompanied by the emission of thermal energy into the atmosphere, which leaves an endothermic peak on the DTA curve, with a minimum within 670–685 °C.

This thermal effect, together with the thermogravimetric index of the release of hydroxyl mass from the sample, serves as a major indicator in the diagnosis of serpentine.

The more intensive the reaction of serpentine dehydration, the higher the orderliness of its crystal structure [2–12]. Another important thermal criterion in the diagnosis of this mineral is the exothermic effect made within ~700–810 °C. This is caused by the destruction of the dehydrated silicate–silicate framework of the serpentine structure. This process of destruction leaves a pronounced exothermic peak in the region of 800 °C on the DTA curve. The intensity of the considered phenomenon is also connected with the degree of the ordering of the mentioned formation; that is, the greater the height of the exothermic peak on the DTA curve, the more perfect the crystalline structure of serpentine. Additionally, on the contrary, the weakly expressed thermal effects in the region of 800 °C are characteristic of defective structures of the described mineral.

The water ejected from the system, in the range of 440~800 °C, is a diagnostic sign of serpentine. The intensity of water released into the atmosphere, within 250~440 °C, could indicate the degree of disorder in the structure of the mineral tested (the more water released into the atmosphere, the more perfect the structure of serpentine) [2–10]. The removal of crystalline (hydroxyl) water from the lattice of serpentine is accompanied by the removal of thermal energy from the system, which leads to a lag in the temperature growth of the sample, concerning the growth of this parameter in the reference crucible. This leads to the formation of a well-defined endothermic peak on the DTA curve, with an extremum in the region of 670 °C.

The thermogravimetric analysis, carried out in the quasi-thermal heating mode, returned the following water contents for these samples: 20.7%, 20.0%, and 21.4%, respectively, which agrees well with the theoretical value (21.6%) of serpentine. The results of the diffractometric and petrographic determinations refer these samples to serpentines with well-ordered crystal structures.

Based on the results of the thermal analysis, it was found that, during weathering, as a result of rearrangement of the silicate framework, the redistribution of the adhesion energy of hydroxyl water with elements of the crystal structure of serpentine occurs. The lattice rearrangement of this system entails a change in its enthalpy. Thus, the DTA curve changes its morphology, which no longer corresponds to serpentine. As the lattice structure of serpentine changes, the mode of water release into the atmosphere changes. The transformation of serpentine into kerolite in its crystal lattice changes the former positions of magnesium and oxygen atoms. This leads to a decrease in the binding energy of hydroxyl groups. It is known that a change in the binding energy of hydrogen oxide in the system leads to a change in the activation energy (E_A) [16]. For the specified mineral phases via the method of Coats A.P. and Redfern J.P., the parameters of E_A were obtained [17]. It was found that, during the transition of serpentine to kerolite, the activation energy of the release of constitutive water (OH) from its structure decreases by 40–60 kJ/mol.

At the Buranovskoye deposit, using the change in curve trajectory, a zone of serpentine transformation into kerolite is well-traced (Figure 7). The subsequent weathering of kerolite leads to the formation of nontronite. Such a transformation is associated with a change in the balance of internal energy of the former formation, which is caused by the recrystallization of its structure [8–10].

According to the thermogravimetric curves of samples 76–83 (Buranovskoye deposit) in the zone of the nontronites, there is an increase in the amount of adsorbed-form H_2O in the structure of ferrous montmorillonites (Fe-montmorillonite), which entails a decrease in constitutional water. This is natural, since, in this thickness of the crust (4–10 m), the kerolite, for the most part, was transformed into nontronite. At the upper levels of the considered zone (samples 76 (4 m) and 77 (5 m)), in the vicinity adjacent to the ocher zone, the tested samples leave information on their differential and thermogravimetric curves, which is not typical for well-ordered nontronites (decreased intensity of the low-temperature effect and rearrangement of masses of differently bonded water). In the rocks sampled higher up in the section, the DTA curve of the samples registers an endothermic manifestation in the region of 330 °C, caused by the release of hydroxyl water into the atmosphere. Such a manifestation is usually a characteristic of the thermal destruction of the goethite, which

is formed as a result of the hypergenic transformation of nontronite by its decomposition. Figure 5 shows that, as the depth of the section decreases to one meter, the magnitude of the peaks left by the DTA and DTG curves changes. At three meters from the surface, sample 75 leaves weakly pronounced effects on these curves, due to equally weak dehydration reactions. However, above this horizon at two meters, sample 74 has deep peaks on its curves, indicating a high degree of hydration of the goethite. Further, within one meter from the surface of the studied sequence, the thermal curves of sample 73 again registers the presence of a weakly developed reaction in the 310 °C region of the same nature as those occurring in the rocks described above. Changes in the morphology of endothermic peaks on the differential curves, as well as the corresponding variation of weight loss values (in the range of 300–350 °C), which indicates a change in the composition of rocks, in favor of the oxides of iron, silicon, calcium, magnesium, and their hydroxyl variations, instead of clay minerals. According to differential and thermogravimetric curves, the products of the final hydrolysis of the considered profile are dominated by the goethites and their aqueous varieties. In the upper part of the weathering crust, the content of iron hydroxides in the samples increases and reaches its maximum in the middle part of the zone, between its lower and upper boundaries. At the upper levels of the section, the content of this mineral decreases. X-ray phase analysis shows that a change in the ratio between the mineral associations orthochrysotile–clinochrysotile–chlorite–talc leads to a change in the intensity of the background scattering measured at line (060), as well as the criteria for the statistical processing of X-ray data. The ratio of the chlorite and chrysotile line intensities shows the increase in chlorite proportion in more transformed friable formations. The change in the elemental composition of serpentinites is illustrated by the level of background scattering. In the initial stage of weathering, an elevated background at the peak (060) is noted, indicating a relatively high iron content. The intensity of the background is almost two times lower in the survey of friable disintegrated sediments, and it is even lower again in the survey of the weathered serpentine. Such patterns of X-ray changes in the transformed crystalline structures can also be traced to other varieties of serpentinite, which is reflected in Figure 7.

Using the numerical criteria (change in interplanar distances) obtained by statistical processing of diffractometry data, it is possible to separate the stages of the beginning of changes in the chemical composition by the ratio of minerals and degree of the disorder, along with the crystallographic directions in the serpentine structure.

The weathering crusts of the Kempirsay massif contain disordered polytype varieties of serpentine minerals. The ratio of intensities and position of reflexe 201 on a diffractogram of unchanged serpentine of deep horizons indicates the presence of a mixture of clino- and ortho-chrysotile. In unchanged serpentines, orthochrysotile prevails; during weathering, the content of the clinochrysotile component increases.

The yypical associations of chrysotile with chlorite, talc, nontronite, chalcedony, opal, iron oxides, hydroxides, and carbonates are distinguished for the diagnostics of weathering zones. Successive stages of weathering are characterized by changes in relative intensities of diffraction reflections of minerals (Figure 8). The criteria of statistical treatments of diffractograms [D_{av} (001), K_v] also change. [D_{av} (001), K_v] is the average value of the interplanar distance of plane (001), which is a crystallographic index. K_v is a coefficient characterizing the degree of variability of properties or mineral crystalline phases, as well as their interplanar parameters or values. Kerolites are characterized by a diffused character of reflexes and increased coefficient of basal interplanar distances d(001). It has been noted that the removal of magnesium from the serpentine lattice is accompanied by a reduction in the unit cell volume. Leaching increases the structural defects and variation coefficient. In the zone of carbonized serpentinites, the d(001) of serpentine decreases, while the degree of structural ordering is preserved.
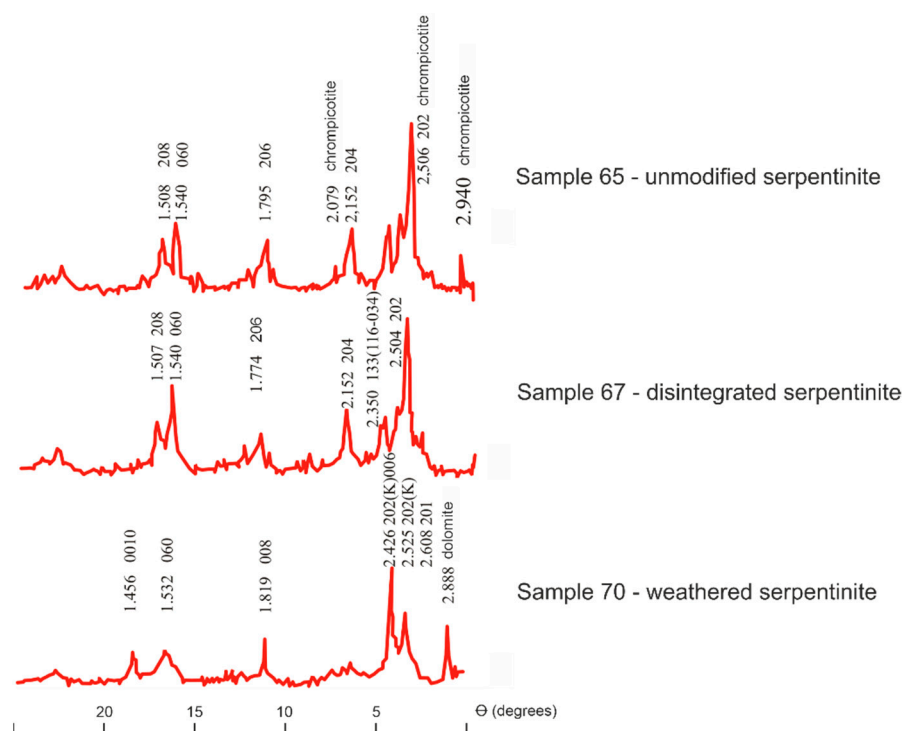
Figure 8. Diffractograms of unmodified, disintegrated, and weathered serpentinites of the Kempirsay massif, Donskoye deposit.

According to microscopic examination, according to X-ray diffractometry (XRD) and the results of differential thermal analysis (DTA and TGA), the following profile of the weathering crust emerges. It characterized by a certain paragenetic characteristic (from bottom to top), i.e., from serpentinites to products of final hydrolysis by the following zones: (1) disintegrated and leached serpentinites, (2) nickel-bearing talcs and saponites, (3) nontronites, and (4) minerals of final hydrolysis (goethite, limonite, periclase, pyrolusite, and hydrated varieties).

The structural features of serpentines, established by X-ray diffraction analysis of a series of samples along the weathering crust profile, may be considered as the criteria for the differentiation of the transformation stages [9,16].

This work shows the staged nature and sequence of the transformation of serpentinite into weathering products (kerolite, nontronite, and ocher) through the change in activation energy values of these minerals. This was calculated by the method presented in [17], using the weight loss (dm) when heating the samples, reaction rate, and temperature intervals (dt °C) of their decomposition. In weathering crusts, the conversion of serpentine to nontronite may proceed to bypass the intermediate metastable kerolite phase. According to Ostwald's rule [18,19], such transformation requires more energy than the transition through the kerolite phase. Hence, the activation energy (E_A) of the direct transformation of serpentine should be higher than E_A, which is necessary for step-by-step transformation.

Based on computer calculations (using the Coats–Redfern method) [16] regarding the kinetics of degradation of hypergenic minerals [2,9], we obtained the activation energy of dehydration and dehydroxylation of weathering products from different areas and depths of the Kempirsay ultramafite massif: E_{A1}—activation energy of serpentine and, respectively, kerolite destruction; E_{A2}—activation energy of dehydroxylation of goethite component; E_{A3}—activation energy of low-temperature dehydration, which is the energy characteristic of the nontronite component of hypergene formation; and $\sum E_A$—sum of these parameters. When comparing the mentioned parameters with the data responsible for the degree of transformation of rocks from the considered borehole, the tendency of decreasing E_{A3} along the section was noted, which indicates a decrease in the bond energy of the OH group in the

structure of serpentine during its hypergenic transformation. The deterioration of hydroxyl bonding in the structure is caused by a decrease in the perfection of the crystal structure—first of serpentine, then of kerolite. As the E_{A3} value decreases along the crustal profile, the growth in E_{A1} is traced, characterizing the process of nontronite structure formation.

Since the weathering products from the presented borehole contain water in their composition, in both molecular and hydroxyl forms, the parameter $\sum E_A$ (obtained by their complete thermal dehydration) can serve as an accessible characteristic of their energy state. In the process of the hypergenic transformation of minerals, according to the scheme serpentine→kerolite→nontronite, the value of the indicated parameter decreases from 248 to 40 kJ/mol. However, above the nontronite zone, the change in $\sum E_A$ occurs in the opposite direction, i.e., in the zone of ocher, the value of the total activation energy increases to ~190 kJ/mol.

The obtained scheme of variation in energy parameter E_A is valid for the case of the consecutive transformations of mineral phases in the weathering profile. It is applicable if the transformation of kerolite, nontronite, and goethite is considered as a single process in the chain of hypergenic transformations. In this case, the change of activation energy in these transitions can be compared to the change in internal and free energy of the crystal structures of the transforming phases. Taking into account these assumptions and based on kinetic parameters of thermal destruction of minerals, thermodynamic constructions were made to illustrate the change in free energy of the system during hypergenic transformations, according to Ostwald's rule [18,19] (Figure 9). The growth in the free energy of the crystal lattice of goethite (hydrogoethite) during its transformation from the structure of nontronite indicates the exothermic nature of the mentioned transformation (Figure 9). The increase in $\sum E_A$ in the samples of the ocher zone, relative to the same parameter from the nontronite zone, indicates that the free energy of the crystal lattice of hydrogoethite and goethite per unit volume of a substance is higher than that of the nontronite structure. Comparing the kinetic parameters of direct transformation of minerals with the parameters of multistage transformation, it follows that the activation energy of the one-stage transition of serpentine into the final weathering product is higher than the sum of activation energies of the adjacent intermediate phases (Figure 9). Consequently, the most preferable way to form hypergenic minerals from parental rocks is step-by-step transformation. The control calculations of crystallochemical parameters of the minerals in question also led to this conclusion.
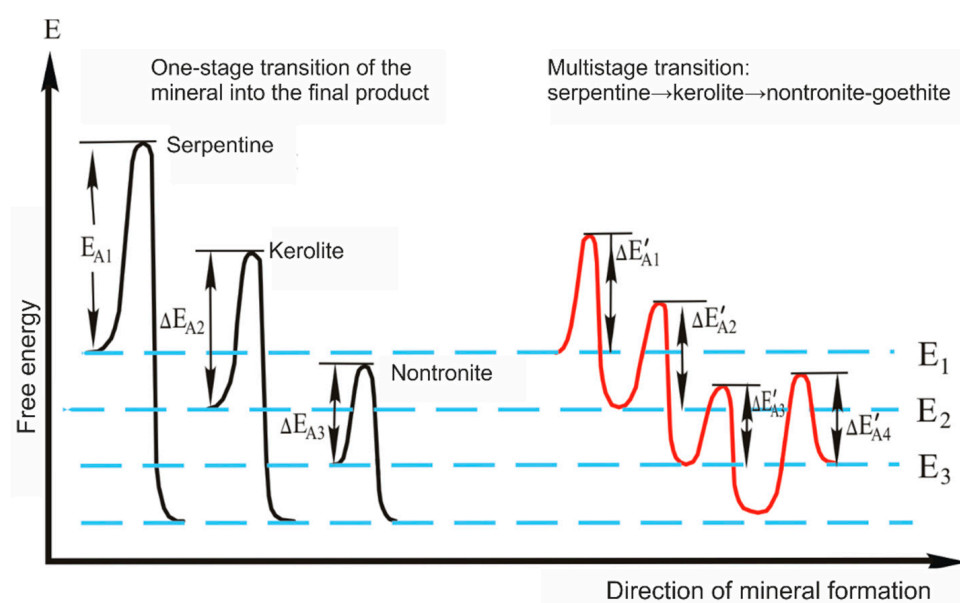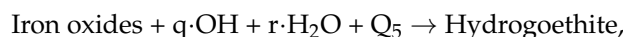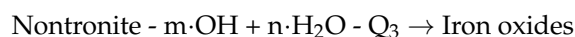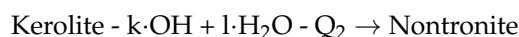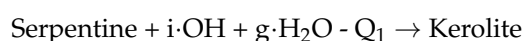

Figure 9. Diagram of changes in the free energy of the system during the transformation of hypergenic minerals in weathering crusts (Ostwald's rule).

As a result of this study, it was found that:

1. In the stages of formation of exogenous products that precede the formation of goethite and hydrogoethite in the studied weathering profiles, nontronites are the most stable. The stability of these minerals is determined by small levels of internal energy, due to which, their further transformation in steady-state environmental conditions is difficult, without an inflow of energy from the outside. Since the ocher zone is located near the surface, bordering the soil cover of the weathering crust, additional energy sources could include flowing infiltration waters, solar energy, the vital activity of microorganisms, including soil bacteria, and the influence of soil-ulmin acids of complex compositions.

For a clear representation of the methods of transformation of the considered minerals, taking into account variations in the heat of their transformation and activation energy barriers of each transition, a thermodynamic scheme of serpentine stage transformation into a final weathering product was made:

$$Serpentine + i{\cdot}OH + g{\cdot}H_2O - Q_1 \rightarrow Kerolite$$

$$Kerolite - k{\cdot}OH + l{\cdot}H_2O - Q_2 \rightarrow Nontronite$$

$$Nontronite - m{\cdot}OH + n{\cdot}H_2O - Q_3 \rightarrow Iron\ oxides$$

$$Iron\ oxides + p{\cdot}OH + Q_4 \rightarrow Goethite$$

$$Iron\ oxides + q{\cdot}OH + r{\cdot}H_2O + Q_5 \rightarrow Hydrogoethite,$$

where, i, g, k, ... , and a are proportionality coefficients; Q_1, Q_2, and Q_3 are the heat released by the system during the transition from the upper energy level to the lower energy level; and Q_4 and Q_5 are the heat spent by the system during the transition from the lower energy level to the upper one.

In this regard, it should be noted that a change in the amount of OH and H_2O leads to the removal from (or inflow to) the system of only a portion of the heat. The change in the remaining heat is governed by variations in the amount of silicon, magnesium, iron, nickel, and other components in the sample. The use of Ostwald's principle to determine the favorable, from the kinetic point of view, methods of the formation of consecutive phases from any structural formation is acceptable, not only in cases of studying natural transformations, but also in laboratory studies of binary systems [18,19].

2. With the help of the above-mentioned scientific instrumental means and methods of research, we have established physical and chemical signs at the level of the state of the crystal structure of minerals, which allows for determining the ore-bearingness of weathering crusts and prospects of formation and accumulation of nickel, iron, magnesium, and other ore components in them.

The patterns of chemical element distribution in the weathering zones of the studied deposits were traced. In serpentinites, the concentration of nickel does not exceed 0.3%. Further down the section, in the zone of kerolitized serpentinites, its quantity increases from 0.5 to 1.0%; in the layers of nontronitized kerolites, it increases up to 1.5%. The maximum concentration of this element is reached in the upper floors of the nontronite zone, at 2.2%. At the levels bordering ocher, the amount of nickel decreases to 1.2%, and in the zone of final hydrolysis, the concentration does not exceed 0.5%. It follows that nickel accumulates in the products of incomplete decomposition at the initial stage of weathering, during the disordering of the serpentine structure. As a result of the destruction of the crystal lattice, new phases are formed: kerolite, chrysotile varieties, and, less often, Fe-montmorillonite. As secondary minerals develop, the intensity of the accumulation of associated nickel and its oxides increases. Further weathering leads to the destruction of chrysotile structures and kerolite with the subsequent development of nontronite. From this point onwards, the deposition of nickel from infiltration solutions proceeds most intensively. Thus, the criteria for the highest concentration of Ni in the products of hypergenesis are kerolite–nontronite associations, whose crystal lattices are disordered (or arrive) at the stage of destruction.

On the mobility of magnesium during the formation of secondary minerals in the considered deposits, it follows that its average content in the studied weathering products is subordinate to the degree of hypergenic transformation of serpentine into new minerals. The greatest amount of this element is concentrated in the host rock itself. As the serpentinite wears away, the amount of magnesium decreases. The amount of aqueous inclusions in the rock also changes. Thus, the leached serpentinite is characterized by a different chemical composition and arrangement of the energy bonds of the H_2O and OH groups (the content of molecular water increases in the crystal lattice by reducing the number of hydroxyls). The amount of magnesium in the formation is reduced to 10%, against the concentration (26%), which is typical for serpentines. Reducing the content of Mg and changing the weight ratios of SiO_2, H_2O, and OH leads to a radical restructuring of this mineral, with its transition to a new formation—kerolite. In this case, instead of the definition of "defective structure of serpentine", it is appropriate to use the phrase "disordered structure of kerolite". The further escape of magnesium from the kerolite structure leads to the destruction of the octahedral lattice layer of this formation and formation of defective bonds in its tetrahedral grid.

At low concentrations of Mg (<10%), serpentine loses silicon. At a critical mass ratio of magnesium to silicon, the state of the structure becomes metastable and disintegrates. The change in magnesium concentration, in the form of its oxide in the weathering zones of Buranovskoye and Shelektinskoye deposits, is noted in Figure 9.

The removal of magnesium from mature weathering products is partially compensated by the introduction of iron. This process is intensified in the upper limits of the nontronite horizons; in the ocher zone, it leads to the intensive accumulation of iron oxides, the content of which (in the products of final hydrolysis) reaches 70% and higher.

The accumulation of trivalent iron in the upper weathering zones is accompanied by a decrease in the silica content in the products. Within the ocher zone, the iron content increases by 2.5 times, compared to the nontronite zone. Destroyed nontronite structures form free oxides or enter as the main component in the crystal lattices of iron minerals (goethite and their hydrated variations).

The study of the Kempirsay nickel deposits shows that they have a two-tier structure, in which the hypergenic upper tier has a continuation, in the form of the lower hydrothermal tier, which agrees with the data of Talovina I. V. [13,19], Lazarenkov V.G., Talovina I.V. et al. [14,15], and, thus, increases the prospects for finding new ore objects at depth.

3. According to the results of thermal research of weathering products of Buranovskoye deposit (well 2250), it has been revealed that, in some fractions with particle sizes < 0.001, 0.001–0.005, 0.005–0.01, 0.01–0.05, and 0.1–0.25 mm, nickel-bearing nontonite and kerolite are predominant (Figure 4). The number of these formations grows nonlinearly from the bottom to the top of the section. Their maximum increase is observed in the near-surface levels of the studied sequence. The greatest amount of nontronite is concentrated in fraction no. V (fraction 0.05–0.1 mm). The above figure shows that, when decreasing the depth of the borehole, the increase in nontronite in the samples grows more intensively than that of kerolite. When reaching the upper limits of the section, four fractions (I, III, IV, and VI) out of the seven studied revealed pure nontronite.

Comparing the gravimetric spectra of the samples from the zone of nontronites and kerolitized serpentinites (Figure 5II) with the diagram of Ni, MgO, and Fe_2O_3 distribution in the weathering crust section of the Buranovskoye deposit (Figure 10), we can trace the dynamics of change in the nickel content in the samples, depending on the rock depth and dispersion of nontronites and kerolites in it. Such an approach, in consideration of the aggregate state and mineral composition of the main rock-forming minerals of weathering cores, together with reconstruction of the mechanism of accumulation in zones of hypergenesis of valuable ore components, may be useful, not only when searching for them geologically, but also in the technology of mining and understanding the concentration of these minerals.
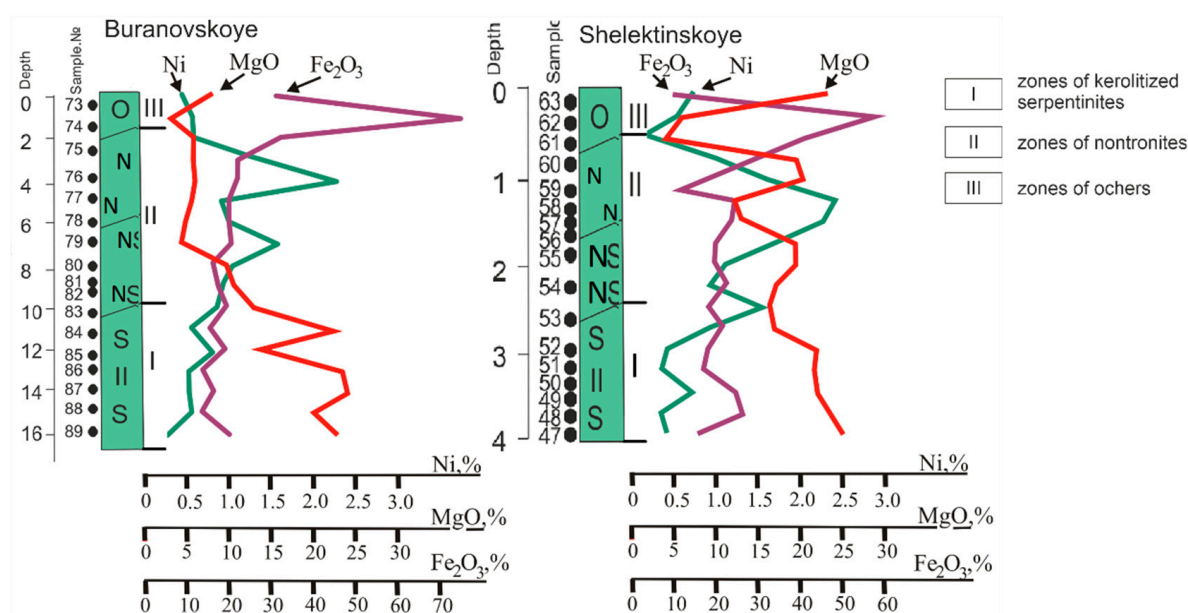
Figure 10. Diagram of Ni, MgO, and Fe_2O_3 distribution in the section of the weathering crust of ultramafic rocks of Buranovskoye and Shelektinskoye deposits, according to thermal and chemical analyses.

5. Discussion of the Results

In the Middle and Southern Urals (Russia), the nickel deposits of the Serov and Ufaleya [14,15,20] weathering crusts differ in structure and mineral composition from those of the Kempirsay ultramafite massif. For the Kempirsay group of deposits, the nickel weathering crust profile is represented by three mineral zones: 1—leached (kerolitized) serpentinites; 2—nontronites; and 3—ochers.

The weathering crusts of the Serov and Ufaley groups have a different mineral profile of chrysotile–pecorite. This is probably due to the different geological, tectonic, and geodynamic positions of the ultramafites [15].

Lateritic nickel deposits are widely understood in Indonesia, the Philippines, Brazil, Cuba, Australia, and New Caledonia. Lateritic nickel is formed in humid tropical climates by the weathering of ultramafic rocks. Nickel is contained in several minerals, such as magnesium oxides (periclase), silicates (serpentines, talc, and chlorites), clay minerals and hydromica, iron oxides, and hydroxides, as well as an extensive group of minor minerals [21–23]. At different depth levels, these minerals can acquire rock-forming significance and act as the main ore mineral. The minerals of nickel-bearing weathering crusts are characterized by their finely crystalline, or even amorphous, structure, with extensive development of mixed-layer mineral species. Serpentinites are the most important industrial minerals in nickel ores of hypergene deposits [21]. Hydrometallurgical [24] and pyrometallurgical [25,26] methods of extraction are used to obtain nickel. Ores with nickel content (less than 1.3% Ni) are subjected to hydrometallurgical treatment. These ores correspond to the nickel-bearing weathering crusts of the Kempirsay ultrabasite massif.

Lateritic nickel deposits are divided into three groups [22,23]: (1) oxide or "limonite" and their hydroxyl differences deposits, with rock-forming goethite; (2) smectite or "clay-mineral" deposits, composed of nickel-bearing clays, such as smectite or nontronite; and (3) water deposits of magnesium silicate, composed mainly of talc and serpentine [27]. The weathering crust of the Kempirsay ultramafite massif corresponds to the second type of clay mineral formation, with an average nickel content of less than 1.3% Ni. The main source of its accumulation in weathering products is serpentinites; the Ni content is about 0.3%. Up in the weathering crust section, the nickel concentration increases in the kerolite zone to 2%; in the nontronite zone, it reaches 2.5%. In the near-surface horizon, the Ni content decreases to 1.2%. At the daytime surface level, in the zone of final hydrolysis,

the presence of Ni does not exceed 0.5%. It was found that the maximum nickel content is confined to the kerolite–nontronite association. In these parageneses, the degree of perfection of the crystalline structure of nontronite is usually low, and the silica–oxygen framework of the kerolite structure is in a disordered state. Thus, our determinations of the mineral and chemical compositions in the studied weathering profiles, as well as the results of calculations of concentrations of valuable ore components in them, can be used as diagnostic signs in the search for (and evaluation of) the reserves of the hypergene ultramafite complexes of ores.

According to their thermodynamics, the hypergenic transformation of serpentinites (Figure 9) and formation of kerolite and nontronite proceed with the decreasing internal energy of their crystal structures (endothermic process), while the decomposition of nontronites to simple oxides occurs with increasing energy (exothermic process). This agrees with the results revealed by Talovina I.V. [20].

6. Conclusions

X-ray diffractometric analysis (XRD) can be used as a rapid diagnostic method for monitoring the extraction of nickel ores from weathering roots for subsequent processing. XRD has been proven as a reliable analytical method for monitoring the mineralogical composition of ores and ore concentrations [20,21].

The results of X-ray structural and thermal analyses of nickel weathering crusts are presented, and the products of hypergenic transformation of ultramafites into disintegrated and leached serpentinites, kerolites, nontronites, and ochers are investigated.

A method of thermodynamic interpretation of the processes of hypergenic transformations is proposed. Data on heat exchange processes, which take place in crystalline structures of transformed minerals, are obtained. These data revealed the energetic (endo- or exothermic) directions of the formation of secondary minerals. With the help of the performed method, the changes in the kinetic parameters of the transformed systems have been established.

The distribution of accompanying trace elements along the weathering crust profile of serpentinites is related to the material composition of the ultramafites. The accumulation of nickel, in commercial concentrations, is confined to nontronite–kerolite clays, and its content is controlled by the state of the crystal structure of these minerals, which ultimately expands the field of searching for new deposits. In the studied weathering crusts, nickel reaches high concentrations in kerolite–nontronite associations. In such nickel-bearing associations, the crystal structures of kerolite and nitronite are usually not distinguished by high degrees of crystal structure perfection.

sincere gratitude to the reviewers and editor of this article for their friendly attitude and constructive comments made.

Conflicts of Interest: The authors declare no conflict of interest.

References

1. Tazhibaeva, P.T.; Ponomarev, D.V. *Weathering Crust of Ultramafic Rocks of Kazakhstan and Useful Minerals*; Science: Almaty, Kazakhstan, 1980; p. 204. (In Russian)
2. Tazhibaeva, P.T. *Minerals of the Ancient Weathering Crust of Kazakhstan*; Science: Almaty, Kazakhstan, 1988; p. 256. (In Russian)
3. Kiselev, A.L.; Kazantsev, M.M.; Gulyaeva, N.A. *Kazakhstan Chrome, Nickel, Cobalt and Vanadium Deposits*; Science: Almaty, Kazakhstan, 1997; p. 158. (In Russian)
4. Brindley, G.W.; Maksimovic, Z. The nature and nomenclature of hydrous nickel-containing silicates. *Clays Clay Miner.* **1974**, *10*, 271–277. [CrossRef]
5. Bekzhanov, G.R.; Koshkin, V.Y.; Nikitchenko, I.I. *Geological Structure of Kazakhstan*; AMR of the Republic of Kazakhstan: Almaty, Kazakhstan, 2000; p. 396. (In Russian)
6. Korobkin, V.V.; Buslov, M.M. Tectonics and geodynamics of the western Central Asian Fold Belt (Kazakhstan Paleozoides). *Rus. Geol. Geoph.* **2011**, *52*, 1600–1618. [CrossRef]
7. Frank-Kamenetsky, V.A.; Kotov, N.V.; Goylo, E.A. *Transformational Transformations of Layered Silicates*; Nedra: Leningrad, Russian, 1983; p. 152. Available online: https://www.geokniga.org/bookfiles/geokniga-1535455563183.pdf (accessed on 10 November 2021). (In Russian)
8. Tazhibaeva, P.T.; Slyusarev, A.P.; Samatov, I.B. Supergene transformation of minerals and ore content of weathering crusts. In *Geology and Metallogeny of Kazakhstan*; Abdullin, A.A., Ed.; Science: Alma-Ata, Russia, 1989; pp. 288–304. (In Russian)
9. Tazhibaeva, P.T.; Slusarev, A.P.; Samatov, I.B. Kinetics of mineral formation and useful minerals in weathering. In Proceedings of the 28th International Geological Congress, Washington, DC, USA, 9–19 July 1989; Volume 3, p. 224. (In Russian).
10. Talovina, I.V. Geochemistry of Supergene Nickel Deposits in the Urals. Abstract of Doctoral Dissertation. National Mineral Resources University "Mining" 2012, p. 38. Available online: https://viewer.rusneb.ru/ru/000199_000009_005054116?page=1&rotate=0&theme=white (accessed on 22 March 2022). (In Russian).
11. Brindley, G.W.; Wan, H.M. Composition, structures, and thermal behavior of nickel-containing minerals in the lizardite-nepouite series. *Am. Miner.* **1975**, *60*, 863–871. Available online: https://pubs.geoscienceworld.org/msa/ammin/article-abstract/60/9-10/863/543147/Compositions-structures-and-thermal-behavior-ofwhite (accessed on 10 March 2022).
12. Setiawan, I.; Febrina, E.; Subagja, R.; Harjanto, S.; Firdiyono, F. Investigations on mineralogical characteristics of Indonesian nickel laterite ores during the roasting process. In Proceedings of the IOP Conference Series: Materials Science and Engineering, Tangerang Selatan, Indonesia, 25–26 September 2019; Volume 541, p. 012038. [CrossRef]
13. International Chronostratigraphic Chart. International Commission on Stratigraphy. 2021/10. Available online: www.stratigraphy.org (accessed on 22 March 2022).
14. Lazarenkov, V.G.; Talovina, I.V.; Beloglazov, I.N.; Volodin, V.I. *Platinum Metals in Supergene Nickel Deposits and Prospects for Their Industrial Extraction*; Nedra: St. Petersburg, Russian, 2006; p. 188. (In Russian)
15. Lazarenkov, V.G.; Talovina, I.V.; Vorontsova, N.I.; Mezentseva, O.P.; Ryzhkova, S.O. Nickel chlorites in the Oxide-Silicate Nickel Deposits of the Urals. *Lith. Min. Res.* **2011**, *46*, 312–320. [CrossRef]
16. Ivanova, V.P.; Kasatov, B.K.; Krasavina, T.N.; Rozinova, Y.L. *Thermal Analysis of Minerals and Rocks*; Nedra: Moscow, Russian, 1974; p. 400. (In Russian)
17. Coats, A.P.; Redfern, J.P. Kinetic parameters of thermogravimetry data. *Nature* **1965**, *3*, 917–920. [CrossRef]
18. Kozlov, V.A.; Samatov, I.B. Thermodynamic criteria for the transformation of mineral forms VO, FeO and MnO under conditions of increasing temperature. *Bull. Nat. Acad. Sc. Rep. Kaz. Geol. Ser.* **2013**, *2*, 91–97. (In Russian)
19. Putnis, A.; McConnell, J.D.C. Principles of Mineral Behaviour. *Geosci. Texts* **1980**, *1*, 272. Available online: https://books.google.kz/books/about/Principles_of_Mineral_Behaviour.html?id=v9CzAAAAIAAJ&redir_esc=y (accessed on 10 November 2021).
20. Talovina, I.V.; Khaide, G. Serpentines of the chrysotile-pecoraite series as genesis indicators of nickel deposits in the Urals weathering crusts. *J. Min. Inst.* **2016**, *221*, 629. [CrossRef]
21. König, U. Nickel Laterites—Mineralogical Monitoring for Grade Definition and Process Optimization. *Minerals* **2021**, *11*, 1178. [CrossRef]
22. Brand, N.W.; Butt, C.R.M.; Elias, M. Nickel laterites: Classification and features. *AGSO J. Aust. Geol. Geophys.* **1998**, *17*, 81–88. Available online: https://research-repository.uwa.edu.au/en/publications/nickel-laterites-classification-and-features (accessed on 10 March 2022).
23. Maurizot, P.; Sevin, B.; Iseppi, M.; Giband, T. Nickel-Bearing Laterite Deposits in Accretionary Context and the Case of New Caledonia: From the Large-Scale Structure of Earth to Our Everyday Appliances. *GSA Today* **2019**, *29*, 4–10. Available online: https://www.geosociety.org/gsatoday/science/G364A/article.htm (accessed on 10 March 2022). [CrossRef]
24. Meshram, P.; Pandey, B. Advanced Review on Extraction of Nickel from Primary and Secondary Sources. *Miner. Process. Extr. Metal. Rev.* **2019**, *40*, 157–193. [CrossRef]

25. Agatzini-Leonardou, S.; Tsakiridis, P.E.; Oustadakis, P.; Karikadis, T.; Katsiapi, A. Hydrometallurgical process for the separation and recovery of nickel from sulphate heap leach liquor of nickeliferrous laterite ores. *Miner. Eng.* **2009**, *22*, 1181–1192. [CrossRef]

26. Tian, H.; Pan, J.; Zhu, D.; Yang, C.; Guo, Z.; Xue, Y. Improved beneficiation of nickel and iron from a low-grade saprolite laterite by addition of limonitic laterite ore and $CaCO_3$. *J. Mater. Res. Technol.* **2020**, *9*, 2578–2589. [CrossRef]

27. Brindley, G.W.; Hang, P. The nature of garnierites—I. Structures, chemical compositions and color characteristics. *Clays Clay Miner.* **1973**, *21*, 27–40. Available online: https://link.springer.com/article/10.1346/CCMN.1973.0210106 (accessed on 10 November 2021). [CrossRef]